# Strong Light-Matter Coupling in Subwavelength Metal-Dielectric Microcavities at Terahertz Frequencies

Y. Todorov,[1,2] A. M. Andrews,[3] I. Sagnes,[2] R. Colombelli,[4] P. Klang,[3] G. Strasser,[3] and C. Sirtori[1]

[1]*Laboratoire "Matériaux et Phénomenes Quantiques," Unversité Paris Diderot-Paris 7, CNRS-UMR 7162, 75013 Paris, France*

[2]*CNRS/LPN, Laboratoire de Photonique et de Nanostructures, Route de Nozay, 91460 Marcoussis, France*

[3]*Solid State Electronics Institute TU Wien, Floragasse 7, A-1040 Vienna, Austria*

[4]*Institut d'Electronique Fondamentale, Université Paris Sud and CNRS-UMR 8622, F-91405 Orsay, France*

(Received 20 February 2009; published 8 May 2009)

We have demonstrated that a metal-dielectric-metal microcavity combined with quantum well intersubband transitions is an ideal system for the generation of cavity polariton states in the terahertz region. The metallic cavity has highly confined radiation modes that can be tuned in resonance with the intersubband transition. In this system we were able to measure a very strong light-matter splitting (the Rabi splitting $2\hbar\Omega_R$), corresponding to 22% of the transition energy. We believe this result to be the first demonstration of intersubband polaritons in the terahertz frequency range.

DOI: 10.1103/PhysRevLett.102.186402 PACS numbers: 71.36.+c, 42.50.Pq, 42.79.Gn, 73.20.−r

One of the most important parameters for light-matter interaction is the dimension of the photonic confinement [1,2] which sets the vacuum electric field amplitude of the cavity photons [3]. So far, devices operating in the light-matter strong coupling regime rely on dielectric confinement, which is, at the best, of the size of the wavelength in the material [4–6]. Instead, if the confinement is provided by two metallic layers, the electromagnetic field can be squeezed, in one direction, into a strongly subwavelength width [7,8]. When the gap between the metals is filled with a two-dimensional electronic system, one obtains a microcavity where a multitude of electrons resonantly interact with an extremely confined photonic mode. In this limit the coupling between light and matter strongly increases, leading to an unexplored regime in which the coupling frequency (the Rabi frequency $\Omega_R$) is one of the dominant characteristic rates of the system [9].

The strong coupling between light and intersubband (ISB) transitions has been observed in the midinfrared wavelength range [10,11], by using AlGaAs/GaAs dielectric waveguides based on total internal reflection. In our work, we illustrate a completely different scheme of light confinement for terahertz wavelengths, in which photons are trapped between two metals separated of a thickness $L$ much smaller than the wavelength $\lambda$ ($\lambda/L \approx 100$). The advantages of the terahertz range are multiple [12]. At these frequencies, the optical constants of metals allow the compression of the electromagnetic field into very small volumes without gigantic Ohmic losses that would spoil the cavity resonance [2]. Moreover, photonic structures in the terahertz region can be realized with relatively simple processing, as the smallest planar features are on the order of $\lambda/4n_r \approx 10$ $\mu$m, with $n_r$ the refractive index of the semiconductor. Finally, for a terahertz transition frequency $\omega_{12}$, the figure of merit $\Omega_R/\omega_{12}$ can be considerably increased, because it scales as $1/\sqrt{\omega_{12}}$ [9]. The unexplored regime, where $\Omega_R/\omega_{12} \geqq 0.5$, has been referred to as the *ultrastrong* coupling regime, and yet unobserved fundamental phenomena, such as the dynamical Casimir effect or the generation of correlated photon pairs, could become accessible in these systems [13].

Planar metallic cavities are widely used to guide electromagnetic radiation in the $\mu$ wave [8] and nowadays are exploited also for semiconductor terahertz quantum cascade lasers [14,15]. For a cavity thickness $L$, smaller than $\lambda/2n_r$, the only existing mode is the fundamental transverse-magnetic $TM_0$ mode with an electric field that is constant throughout the cavity. The vacuum Rabi frequency is then written [1]

$$\Omega_R = \sqrt{\frac{\pi e^2}{4\pi\varepsilon_0 n_r^2 m^*}\frac{f_{12}N_{\mathrm{QW}}(N_1 - N_2)}{L}}. \quad (1)$$

Here $e$ is the electron charge, $m^*$ is the electron effective mass, $\varepsilon_0$ is the electric constant, $f_{12}$ is the oscillator strength of the electronic transition coupled with the cavity mode, $N_{\mathrm{QW}}$ is the number of quantum wells (QWs), and $N_1 - N_2$ is the population difference between the two subbands. When $\Omega_R$ is larger than the damping rates of both the transition and cavity, the eigenmodes of the system are linear combinations of matter and light states, called *intersubband polaritons* [1,16]. The energy degeneracy is lifted, and the new eigenvalues are separated by the Rabi splitting $2\hbar\Omega_R$, which can be revealed experimentally by conducting spectral measurements.

Our photonic design is presented in Fig. 1. The semiconductor material containing the QWs is sandwiched between a planar metallic mirror and a metallic rectangular strip grating with period $p$ and strip width $s$. The $TM_0$ mode is contained between the strips and the planar mirror. As will be explained later in the text, the grating structure both defines a lateral photonic confinement and allows an

 

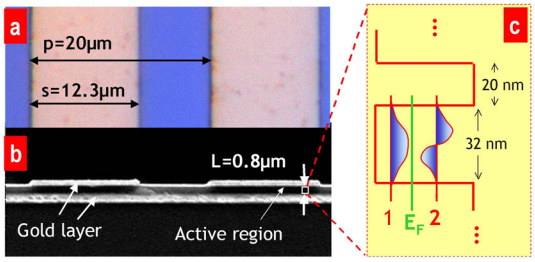


FIG. 1 (color online). The photonic structure used in our experiments. (a) Optical microscope top view of the rectangular metallic grating—with typical dimensions. (b) Scanning electron micrograph of the cleaved facet of the structure. The top and bottom metallic layers are, respectively, 0.4 and 1 $\mu$m thick. The bottom metallic layer is also used to bond the sample on a GaAs host wafer. (c) Schematics of the active layer, containing 15 repetitions of the GaAs/AlGaAs quantum well. The first two energy levels of the wells are separated of 14.5 meV, corresponding to a frequency of 3.5 THz.

efficient coupling of free space photons into the double-metal regions. A major advantage of our structure is that it allows the observation of intersubband polaritons for light under normal incidence, whereas in all previous reports the experiments were performed only at almost grazing incidence, close to the substrate light cone [10,11].

The 32-nm-thick GaAs QWs, grown by molecular beam epitaxy, have a fundamental transition of $\omega_{12}/2\pi = 3.5$ THz ($\lambda = 85.7$ $\mu$m). With 20-nm-thick $Al_{0.15}Ga_{0.85}As$ barriers and $N_{QW} = 15$ well-barrier repetitions, the total thickness of the structure is only $L = 0.8$ $\mu$m. This strongly subwavelength value guarantees single $TM_0$ mode operation in the whole frequency range of interest (up to 9 THz). Note that, in the direction perpendicular to the metal layers, the photon wavelength ($\lambda = 85.7$ $\mu$m) has a high confinement factor $\lambda/n_r L$ on the order of $\approx 30$. Since the $TM_0$ mode has no cutoff frequency, in principle, $L$ can be further reduced to values where only one or two QWs would be needed to achieve the strong coupling regime. The QWs are Si-doped with a sheet density of $5 \times 10^{10}$ cm$^{-2}$. This corresponds to a Fermi level of 1.8 meV at $T = 0$ K, so that all of the carriers will populate only the fundamental subband at low temperatures.

The optical response of the cavities is studied in reflectometry measurements, where the $p$-polarized beam from the Globar lamp of a Bruker Fourier transform interferometer is focused on the device at 45° incidence through a polarizer. The reflected beam is refocused by a pair of confocal $f/2$ parabolic mirrors onto a Si bolometer detector cooled at 4.5 K. The absolute reflectivity is obtained by dividing the obtained spectra on a reference spectrum taken from an unpatterned gold surface. The spectra at $T = 300$ K show no evidence of ISB absorption since the carriers are thermally excited on many subbands. This allows us to characterize the system as an empty cavity. The spectrum of a cavity with period $p = 20$ $\mu$m and strip width $s = 9.6$ $\mu$m is shown in Fig. 2(a), upper panel. In this spectrum, three reflectivity dips, labeled by the integer $K = 1, 2, 3$, are visible. The grating period $p$ is smaller than the wavelength of the incident light, and hence the only diffracted order is the 0th order specular reflection. The dips indicate resonant absorption of the incident radiation due to the excitation of cavity modes [17,18]. The features between 8 and 9 THz are related to the reststrahlen band of the semiconductor. Systematic studies with different periods $p$ and strip widths $s$ show that the resonant frequencies $\nu_K$ of the dips are independent on $p$ but shift regularly with $s$. In Fig. 2(a), we have plotted $\nu_K$ as a function of the quantity $1/s$, which, when multiplied by the light velocity $c$, has units of a frequency. Clearly, $\nu_1$ has a linear dependence with $1/s$. For $K = 2, 3$ the dependence is no longer linear due to the anomalous change of the refractive index for frequencies approaching the reststrahlen band. Therefore, it can be assumed that in the lateral direction the structure simply behaves as a set of independent Fabry-Perot resonators with frequencies:

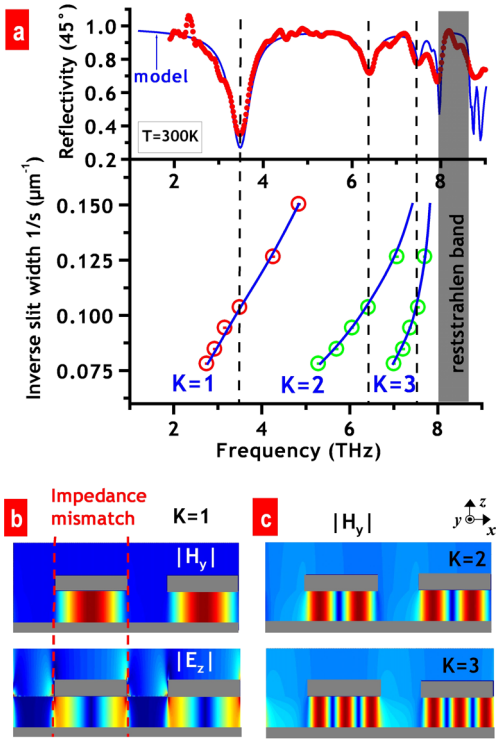


FIG. 2 (color online). (a) Upper panel: Reflectivity spectra of the cavity at a 45° angle of incidence. Lower panel: Position of the three reflectivity minima $K = 1$–3 plotted in an inverse slit $1/s$-frequency diagram. Red dotted curve: Experiment. Blue straight curve: Numerical model. (b) Spatial distribution of the electromagnetic field components $|H_y|$ and $|E_z|$ for the $K = 1$ resonance. Note that the field goes to zero beyond the lines of impedance mismatch; therefore, the different double-metal regions are uncoupled. (c) Spatial distribution of $|H_y|$ for the $K = 2, 3$ resonances. The integer $K$ counts the number of field maxima of the standing wave pattern of $|H_y|$.

$$\nu_K = \frac{cK}{2n_M s}, \tag{2}$$

where $n_M$ is the effective modal index. This picture is consistent with an electromagnetic model, presented in Ref. [18], which reproduces well the reflection curves (blue straight line) [19]. The lateral Fabry-Perot effect arises because of the strong impedance mismatch between the single-metal and double-metal regions which carry the $TM_0$ mode. The impedance mismatch, enhanced in our structure by the strongly subwavelength thickness $L$ of the semiconductor layer, hinders the coupling between the resonators [20]. This is also shown in the contour plots of the relevant electromagnetic field components in Fig. 2(b).

These Fabry-Perot resonances are similar to those arising in a single slit or a periodic array of slits perforated in a metallic film of finite thickness [7,21–23]. Recently, these systems have been extensively studied in connection with the phenomena of extraordinary optical transmission discovered by Ebbesen *et al.* [22]. Scaling the result of Ref. [23] to our structure, we were able to reproduce the rather high effective modal index ($n_M \approx 4.6$ for $K = 1$) extracted by comparing measurements with Eq. (2).

Although the resonant frequencies are independent from the period $p$, the periodicity of the system plays a crucial role in the efficient coupling of the incident photons into the cavities through the grating near field. Indeed, in the case of a subwavelength grating $p < \lambda$, the diffraction generates a set of evanescent orders, closely confined in the vicinity of the grating surface [24]. These evanescent waves, propagating along the grating surface, mediate the energy transfer from the incident plane wave to the tightly confined $TM_0$ modes in the double-metal regions. Numerical modeling shows that the energy transfer is greatly enhanced for shorter periods, which enabled us to achieve very high coupling efficiencies ($\approx$60%). This concept could therefore be applied for building efficient intersubband detectors.

Strip widths $s$ have been chosen so that the frequency of the $K = 1$ mode can be swept in the 2.5–5 THz range [Fig. 2(a)], where the ISB absorption occurs. The absorption is turned on by lowering the temperature which populates predominantly the lowest subband of the QWs. In accordance with Eq. (1), this results in an increased Rabi splitting and the appearance of ISB polaritons. Spectra as a function of the temperature are presented in Fig. 3, where we compare an unprocessed reference sample with a microcavity sample. In the first [Fig. 3(a)] we probe the bare QW absorption in a multipass transmission experiment, whereas in the second [Fig. 3(b)] we show the reflection spectra of a sample fully processed into a cavity with $\nu_{K=1}$ close to the expected absorption.

In the multipass experiment of Fig. 3(a), a transmission dip appears as the temperature is lowered, the signature of a progressively increasing ISB absorption. At $T = 6$ K the absorption feature is centered at 3.66 THz, with a FWHM

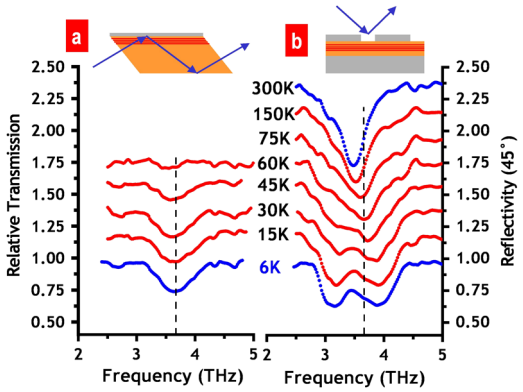


FIG. 3 (color online). (a) Transmission measurements for different temperatures of the quantum well absorption region. The top surface of the sample is fully covered with gold to enhance the terahertz electric field at the metal-semiconductor interface. The terahertz radiation is injected from a 45° polished facet and reaches the quantum well region through the substrate. (b) Reflectivity measurements for different temperatures of the cavity with strip width $s = 9.6$ $\mu$m, nearly resonant with the quantum well absorption (dashed line).

of 0.5 THz. We attribute this rather high value to the donors located inside the QW. The absorption peak shifts slightly with temperature ($\approx$0.1 THz) due to depolarization effects [25]. The absorption disappears at temperatures higher than 70 K, thus justifying the bare cavity studies at room temperature presented above.

In the cavity-processed sample [Fig. 3(b)], the $K = 1$ mode splits into two reflectivity features situated on both sides of the bare QW absorption (indicated by a dashed line). Moreover, the coupling strength of the optical resonance, defined as the area of the reflectivity dip at $T = 300$ K, is almost evenly distributed between the two reflectivity features at $T = 6$ K. These are unambiguous evidences of the strong light-matter coupling regime, the two dips corresponding to the ISB polariton states [1,16].

To further confirm the strong light-matter coupling regime, we have performed low temperature ($T = 4.5$ K) reflectometry measurements by varying the cavity detuning (different strip width $s$). In Fig. 4(a), we present the spectra for three different cavities: one that is redshifted ($s = 8.4$ $\mu$m) with respect to the bare absorption, one in resonance ($s = 9$ $\mu$m), and a blueshifted one ($s = 10.4$ $\mu$m). The bare absorption is always situated between the two reflectivity dips. Figure 4(b) shows the full dispersion in the frequency $-1/s$ diagram. Clearly, the $K = 1$ mode is split into two polaritonic branches with the characteristic anticrossing behavior [1]. The $K = 2$ and $K = 3$ modes appear unaffected as they are considerably detuned from the absorption. Nevertheless, they are blueshifted with respect to those at 300 K due to the temperature variation of the refractive index.

The continuous blue lines in Fig. 4(b) are reflectivity simulations that now take into account the ISB absorption

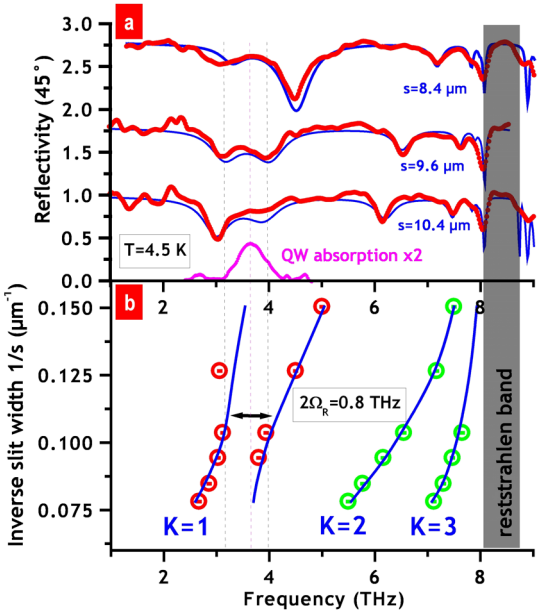


FIG. 4 (color online). (a) Low temperature reflectivity spectra of three cavities, with modes that are, respectively, redshifted ($s = 8.4\ \mu$m), nearly resonant ($s = 9.6\ \mu$m), and blueshifted ($s = 10.4\ \mu$m) with respect to the intersubband absorption. The bare absorption peak from Fig. 3(a) [− log(transmission)] is also shown and has been rescaled for clarity. (b) The dispersion diagram of the system at $T = 4.5$ K. The $K = 1$ mode is split into two polaritonic branches, with minimal energy separation $2\Omega_R/2\pi = 0.8$ THz. The blue continuous lines are our simulations.

through a Drude-Lorentz dielectric tensor, which is a function of the electronic sheet density, as described in Ref. [26]. The experimental results are very well reproduced with the nominal value $N_1 - N_2 = 5 \times 10^{10}$ cm$^{-2}$. The data in Fig. 4(b) allow one to determine precisely a Rabi splitting $2\Omega_R/2\pi = 0.8$ THz at the anticrossing point. This is close to the value 0.9 THz predicted from Eq. (1), using $f_{12} = 0.96$ (the oscillator strength of the fundamental transition of an infinite QW [25]). The value of 0.8 THz is already a significant fraction, 22% of the ISB frequency $\omega_{12}/2\pi = 3.6$ THz.

We believe that these results, which are to our knowledge the first experimental evidence of cavity polaritons at terahertz frequencies, will open a path for the exploration of new optoelectronic devices operating in the strong- and ultrastrong-coupling regimes. In addition, the electronic density in the cavity can be easily controlled by a static electric field [27]. Such a device, in which the photonic confinement may even reach the size of the electronic wave function, could therefore connect the world of semiconductor integrated electronics [28] with that of quantum optics.

We thank C. Ciuti and S. De Liberato for useful discussions and Y. Chassagneux for technical help. We gratefully acknowledge support from the French National Research Agency through the programs ANR-06-NANO-047 MetalGuide and ANR-05-NANO-049 Interpol and from the Austrian Science Fund (FWF).

[1] *Proceedings of the International School of Physics Enrico Fermi, Course CL*, edited by B. Deveaud, A. Quattropani, and P. Schwendimann (IOS Press, Amsterdam, 2003).
[2] S. Maier, Opt. Quantum Electron. **38**, 257 (2006).
[3] Y. Yamamoto, F. Tassone, and C. Cao, *Semiconductor Cavity Quantum Electrodynamics* (Springer-Verlag, Berlin, 2000).
[4] J. P. Reithmaier *et al.*, Nature (London) **432**, 197 (2004).
[5] T. Yoshie *et al.*, Nature (London) **432**, 200 (2004).
[6] J. Kasprzak *et al.*, Nature (London) **443**, 409 (2006).
[7] H. T. Miyazaki and Y. Kurokawa, Phys. Rev. Lett. **96**, 097401 (2006).
[8] A. P. Hibbins, J. R. Sambles, C. R. Lawrence, and J. R. Brown, Phys. Rev. Lett. **92**, 143904 (2004).
[9] C. Ciuti, G. Bastard, and I. Carusotto, Phys. Rev. B **72**, 115303 (2005).
[10] D. Dini, R. Kohler, A. Tredicucci, G. Biasiol, and L. Sorba, Phys. Rev. Lett. **90**, 116401 (2003).
[11] L. Sapienza *et al.*, Phys. Rev. Lett. **100**, 136806 (2008).
[12] This frequency region is loosely defined between 1 and 10 THz and is equivalent to the wavelength range between 30 and 300 $\mu$m.
[13] C. Ciuti and I. Carusotto, Phys. Rev. A **74**, 033811 (2006).
[14] B. Williams *et al.*, Appl. Phys. Lett. **83**, 2124 (2003).
[15] J. Fan *et al.*, Opt. Express **14**, 11 672 (2006).
[16] A. Liu, Phys. Rev. B **55**, 7101 (1997).
[17] A. P. Hibbins *et al.*, Phys. Rev. B **74**, 073408 (2006).
[18] Y. Todorov and C. Minot, J. Opt. Soc. Am. A **24**, 3100 (2007).
[19] For metals, we use a frequency-dependent Drude dielectric constant $\varepsilon(\nu) = (1\text{–}1.52) \times 10^6/\nu(\nu - i16)$, with $\nu$ in terahertz.
[20] We have numerically verified that for very short period $p$ ($s/p \approx 0.9$) the cavities become coupled.
[21] J. A. Porto, F. J. Garcia-Vidal, and J. B. Pendry, Phys. Rev. Lett. **83**, 2845 (1999).
[22] T. W. Ebbesen *et al.*, Nature (London) **391**, 667 (1998).
[23] R. Gordon, Phys. Rev. B **73**, 153405 (2006).
[24] *Electromagnetic Theory of Gratings*, edited by R. Petit (Springer-Verlag, Berlin, 1980).
[25] *Intersubband Transitions in Quantum Wells: Physics and Device Applications I*, edited by H. C. Liu and F. Capasso (Academic Press, San Diego 2000).
[26] L. Wendler and T. Kraft, Phys. Rev. B **54**, 11 436 (1996).
[27] A. A. Anappara *et al.*, Appl. Phys. Lett. **87**, 051105 (2005).
[28] R. Chau *et al.*, Nature Mater. **6**, 810 (2007).